

Short Communication

## **Li<sub>4</sub>Ti<sub>5</sub>O<sub>12</sub>@N-Doped Carbon Composites as Anode Materials for Lithium Ion Batteries**

Lian Liu,<sup>II</sup> Chen-Ru Yang,<sup>II</sup> Qi Luo, Ping Wang, Jiang-Jiang Gu<sup>\*</sup> and Fei-Fei Cao

College of Science, Huazhong Agricultural University, Wuhan, 430070, People's Republic of China

<sup>\*</sup>E-mail: [jiangjianggu@mail.hzau.edu.cn](mailto:jiangjianggu@mail.hzau.edu.cn)

<sup>II</sup>L.L. and C-R.Y. contributed equally.

Received: 4 February 2018 / Accepted: 3 April 2018 / Published: 10 May 2018

Li<sub>4</sub>Ti<sub>5</sub>O<sub>12</sub> is considered a promising anode material for lithium ion batteries because of its zero-strain insertion. However, this material is difficult for widespread application due to its shortage of electronic and ionic conductivity. Herein, we reported a facile hydrothermal combined calcination method to synthesize Li<sub>4</sub>Ti<sub>5</sub>O<sub>12</sub>@nitrogen-doped carbon (LTO@NC) composites by using urea as the nitrogen and carbon sources. The results of electrochemical experiments showed that the LTO@NC composites exhibited a high initial capacity of 194.3 mA h g<sup>-1</sup>, an increased specific capacity and an improved rate performance. This could be ascribed to the N-doped carbon coating that enhanced the electronic conductivity and decreased the polarization of the material and the reduced particle size that hydrothermally shortened the diffusion path of Li<sup>+</sup>.

**Keywords:** Li<sub>4</sub>Ti<sub>5</sub>O<sub>12</sub>; N-doped carbon; Anode materials; Lithium-ion batteries

### **1. INTRODUCTION**

The abundance of traditional energy resources leads to many serious environmental and social problems, such as global warming, ecological or environmental degradation and a shortage of resources. Thus, it is urgent for us to find an alternative energy source that environmentally friendly [1]. The lithium ion battery is a promising alternative because of its various advantages, such as high energy density, high operating voltage, no memory effect and long cycle life. This new type of energy source is widely applied in portable electronic devices and electric vehicles. Moreover, it has been proposed for application in hybrid electric vehicles (HEVs), large-scale energy storage and so on [2, 3].

Li<sub>4</sub>Ti<sub>5</sub>O<sub>12</sub>, with its stable and compact spinel structure, is considered a promising anode material for lithium ion batteries. Its relatively high and stable operating voltage (1.55 V vs. Li/Li<sup>+</sup>)

can avoid the formation of a solid electrolyte interphase (SEI) layer. Its zero-strain property provides excellent cycling performance and a remarkable lithium ion diffusion coefficient ( $2 \times 10^{-8} \text{ cm}^2 \text{ s}^{-1}$ , approximately ten times that of carbon materials). However, the widespread application of  $\text{Li}_4\text{Ti}_5\text{O}_{12}$  is hindered by its low electronic conductivity (approx.  $10^{-13} \text{ S cm}^{-1}$ ) and moderate  $\text{Li}^+$  diffusion coefficient ( $10^{-9}$ – $10^{-13} \text{ cm}^2 \text{ s}^{-1}$ ) [4, 5]. Thus, great efforts have been made to solve these problems: (1) Porous  $\text{Li}_4\text{Ti}_5\text{O}_{12}$  materials were prepared to increase the lithium insertion capacity [6]. (2) The size of the  $\text{Li}_4\text{Ti}_5\text{O}_{12}$  material was reduced to shorten the diffusion path of lithium ions [7]. (3) Multivalent metal ions were doped into  $\text{Li}_4\text{Ti}_5\text{O}_{12}$  materials to improve the conductivity [8, 9]. (4) Surface modification was used to improve the conductivity of  $\text{Li}_4\text{Ti}_5\text{O}_{12}$  with conductive layers, such as highly conductive carbon and metal/metal nitrides [10-13].

Carbon is considered the most popular candidate to coat  $\text{Li}_4\text{Ti}_5\text{O}_{12}$  because of its favorable electrical conductivity. At present, the commonly used carbon sources include glucose [14], sucrose [15, 16] and polyvinyl alcohol [17]. Zhu et al. used a spray drying method combined with high-temperature annealing to prepare carbon-coated (C-coated) LTO nanoporous microspheres, which effectively enhanced the electrochemical performance [18]. Moreover, the introduction of nitrogen into the carbon structure can increase the interfacial stability of carbon and provide more active sites, which can further improve the electrical conductivity [19, 20]. Herein, we reported a facile hydrothermal combined calcination strategy to fabricate  $\text{Li}_4\text{Ti}_5\text{O}_{12}$  composites coated with a N-doped carbon layer by using urea as a nitrogen and carbon source. The electrochemical performance of this material was tested as the anode electrode in a half-cell. The results showed that the introduction of a N-doped carbon coating layer could significantly improve the electrochemical performance of a  $\text{Li}_4\text{Ti}_5\text{O}_{12}$ -based material.

## 2. EXPERIMENTAL SECTION

### 2.1 Synthesis of $\text{Li}_4\text{Ti}_5\text{O}_{12}$

$\text{LiOH} \cdot \text{H}_2\text{O}$ , butyl titanate ( $\text{Ti}(\text{OC}_4\text{H}_9)_4$ ), urea ( $\text{Co}(\text{NH}_2)_2$ ) and ethanol were purchased from Sinopharm Chemical Reagent Beijing (China) Co., Ltd. They were analytical grade and used directly without any further refinement.

First, 5 mmol  $\text{LiOH} \cdot \text{H}_2\text{O}$  and 6 mmol  $\text{Ti}(\text{OC}_4\text{H}_9)_4$  ( $\text{Li}/\text{Ti}=1:1.3$ ) were thoroughly dissolved in 50 mL ethanol with stirring for 12 h under ambient temperature, and the solution gradually became milky white. Then, 50 mL deionized water was added into this reaction system, followed by vigorous stirring for 1-2 min. The obtained moisture was transferred into a stainless steel reactor and immediately heated to 180 °C in an oven and kept for 36 h. After cooling to ambient temperature naturally, the  $\text{Li}_4\text{Ti}_5\text{O}_{12}$  precursor was obtained after washing with deionized water and ethanol several times, followed by centrifugal separation (9000 r/min). Then, the precursor was dried in an oven at 80 °C. Finally, the  $\text{Li}_4\text{Ti}_5\text{O}_{12}$  precursor was annealed in a tube furnace at 600 °C for 6 h under an Ar atmosphere with a heating rate of  $5 \text{ }^\circ\text{C min}^{-1}$ . After that,  $\text{Li}_4\text{Ti}_5\text{O}_{12}$  (LTO) was obtained.

## 2.2 Synthesis of N-doped carbon-coated $\text{Li}_4\text{Ti}_5\text{O}_{12}$

First, 200 mg LTO and 10 mg urea were dispersed in ethanol through ultrasonication for 30 min and dried in an oven at 80 °C. Then, the composite was heated to 350 °C for 3 h with a heating rate of 5 °C  $\text{min}^{-1}$  under an Ar atmosphere. The final product, nitrogen-doped carbon-coated  $\text{Li}_4\text{Ti}_5\text{O}_{12}$  (LTO@NC) was obtained.

## 2.3 Structure and Morphology Characterizations

The crystalline structure of the material was studied by powder X-ray diffraction (XRD, JDX-10P3A) with a filtered Cu  $K\alpha$  radiation source. The morphology of the material was characterized by scanning electron microscopy (SEM, JEOL 6701F). The X-ray photoelectron spectroscopy (XPS) of the material was recorded on an ESCA Lab 250Xi spectrometer (Thermo Scientific).

## 2.4 Electrochemical Evaluations

The electrochemical tests were carried on coin-type CR 2032 cells that were assembled in an argon-filled glovebox (Mikrouna, Super (1220/750)). The working electrode was fabricated by depositing the mixed slurry of LTO@NC, Super P and PVDF binder in N-methyl-2-pyrrolidone (NMP) solvent with a weight ratio of 80:10:10 onto Cu foil and dried at 80 °C in a vacuum oven for 12 h. A lithium foil was used as the counter electrode, and a glass fiber (GF/D) membrane (Whatman) was used as the separator. The electrolyte was 1 M  $\text{LiPF}_6$  dissolved in a mixed solvent of ethylene carbonate (EC), dimethyl carbonate (DMC) and diethyl carbonate (volume ratio 1:1:1). The charge/discharge tests were performed between 1.0 and 3.0 V (vs.  $\text{Li}^+/\text{Li}$ ) with a Land CT2001A battery tester (Wuhan Land Electronic Co. Ltd., China).

## 3. RESULTS AND DISCUSSION

The crystalline structure of the product was confirmed by the X-ray diffraction. Figure 1a shows the XRD patterns of the as-prepared LTO and LTO@NC. It can be seen that the XRD pattern of the as-prepared LTO shows not only characteristic diffraction peaks of the spinel  $\text{Li}_4\text{Ti}_5\text{O}_{12}$  (JCPDS No. 49-0207, space group  $\text{Fd}\bar{3}\text{m}(227)$ ,  $a=8.36 \text{ \AA}$ ), which can be indexed to the (111), (311), (400), and (440) planes and so on, but also two significant peaks at 27.45 ° and 56.6 ° corresponding to rutile  $\text{TiO}_2$  (JCPDS No. 21-1276, space group  $\text{P}42/\text{mmn}$ ,  $a=b=4.60 \text{ \AA}$ ,  $c=2.96 \text{ \AA}$ ). In addition, the peak appearing at 25.30 ° (\*) is the diffraction peak of  $\text{Li}_2\text{TiO}_3$ , which indicates that the as-prepared LTO is not pure when the atomic ratio of Li/Ti is 1:1.3. The average particle size of the as-prepared LTO is approximately 21 nm, which is calculated by Scherrer's formula.

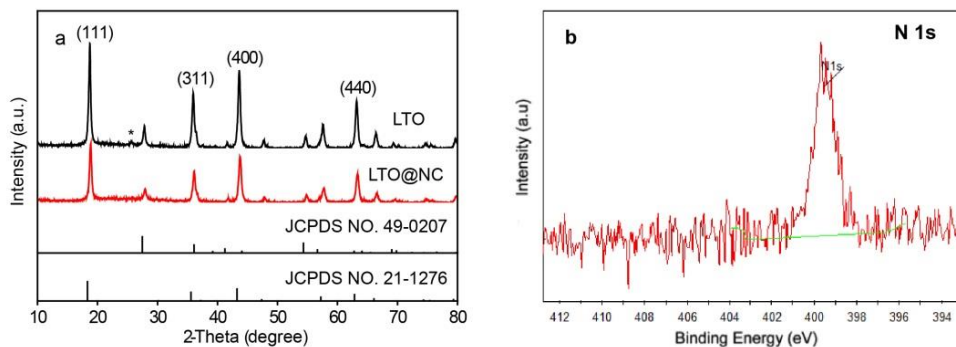


**Figure 1.** (a) XRD patterns of LTO and LTO@NC; (b) N 1s XPS spectrum of LTO@NC.

The XRD pattern of LTO@NC shows that the coating of the nitrogen-doped carbon layer does not change the crystalline structure of the pristine LTO. The peak at  $25.3^\circ$  (\*) disappears, which may be interpreted as the combination of  $\text{Li}_2\text{TiO}_3$  and  $\text{TiO}_2$  under the reducing atmosphere provided by the  $\text{NH}_3$  decomposed from urea [21]. The average particle size of the LTO@NC is 22 nm (calculated by Scherrer's formula), which is slightly larger than that of LTO, indicating that the nitrogen-doped carbon layer may have coated on LTO successfully. Figure 1b shows the N 1s XPS spectrum of LTO@NC, which indicates that nitrogen is indeed doped in the carbon layer.

As displayed in Figure 2, the powder of LTO (Figure 2a) is white, while the powder of LTO@NC (Figure 2b) is dark gray, which can be attributed to the addition of the N-doped carbon coating layer. It is obviously seen from the SEM images that LTO without N-doped carbon coating (Figure 2c) is composed of inordinate nanoparticles, nanotubes and flakes. However, LTO@NC exhibits an ordinate morphology of nanosheets, but no change in the original morphology of LTO (Figure 2d). This may be due to the tiny LTO nanoparticles growing into nanosheets in a certain spatial orientation during the calcination process with urea [22].

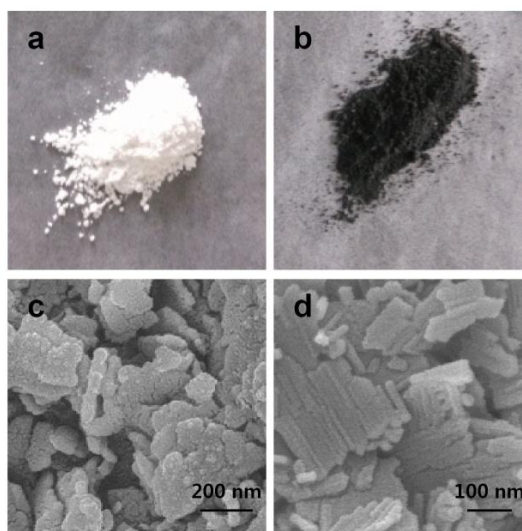


**Figure 2.** The photographs of LTO (a) and LTO@NC (b); the SEM images of LTO (c) and LTO@NC (d).

Figures 3a and 3c show the charge/discharge curves of LTO and LTO@NC at the 4<sup>th</sup>, 5<sup>th</sup> and 6<sup>th</sup> cycles under 0.2 C with the voltage windows of 1.0-3.0 V (vs. Li<sup>+</sup>/Li). Figures 3b and 3d show the charge/discharge curves at the 74<sup>th</sup>, 75<sup>th</sup>, and 76<sup>th</sup> cycles after cycling at different rates for ten laps back to 0.2 C. It is obvious that there is a broad voltage plateau at 1.5 V with polarization. After cycling at high rates, the polarization of both two materials decreases, especially for LTO@NC. A significant stable plateau appears for LTO@NC, but LTO still remains polarized, which represents an improvement in the kinetics for the LTO@NC sample [23]. This result illustrates that the N-doped carbon layer can significantly improve the electronic conductivity and reduce the polarization of the material for further enhancing the electrochemical performance of LTO@NC, which was also demonstrated in other works [24, 25]. In addition, there is no characteristic voltage plateau of TiO<sub>2</sub> (1.8 V), which may be due to its minimal content that does not affect the performance of the whole material.

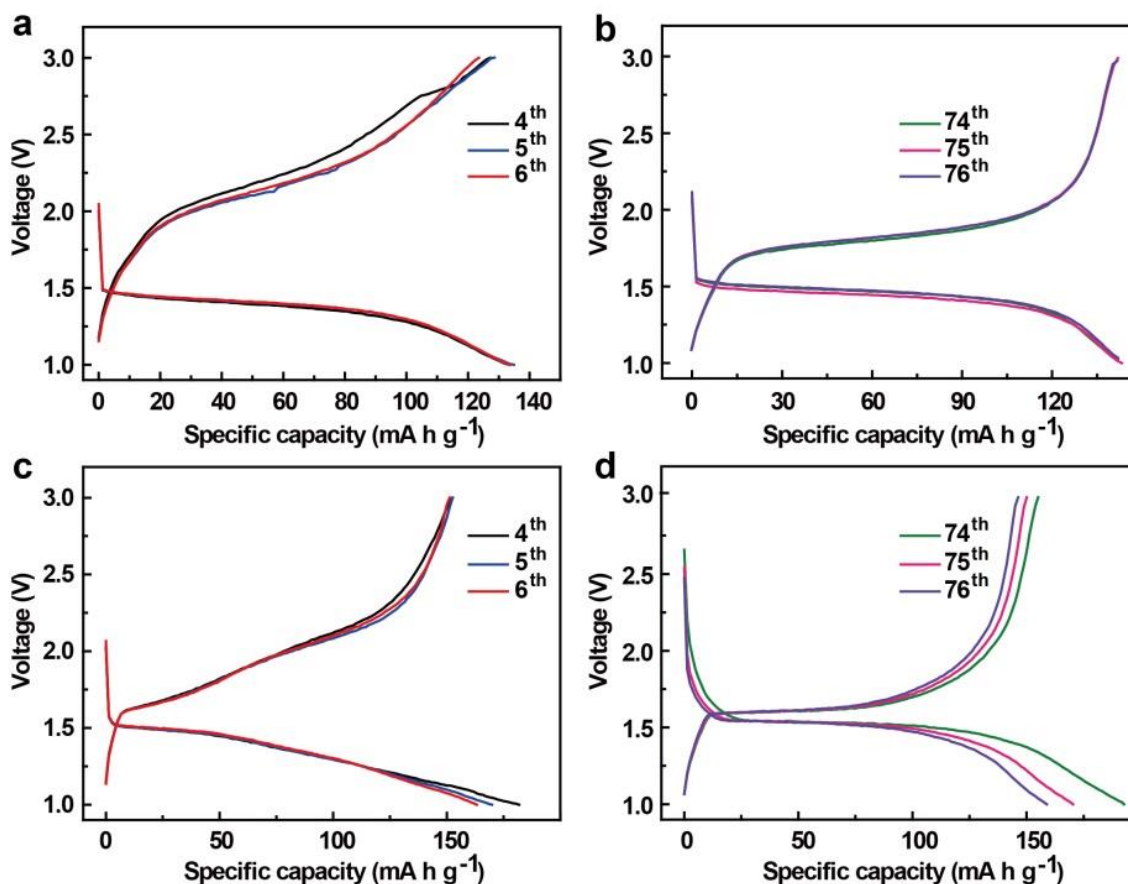


**Figure 3.** The charge/discharge curves of LTO (a) and LTO@NC (c) at the 4<sup>th</sup>, 5<sup>th</sup>, and 6<sup>th</sup> cycles; the charge/discharge curves (back to 0.2 C) of LTO (b) and LTO@NC (d) after cycling at different rates.

It is worth noting that the as-prepared LTO has a charge capacity of 145 mA h g<sup>-1</sup> after the 6<sup>th</sup> cycle, which is higher than that of commercial Li<sub>4</sub>Ti<sub>5</sub>O<sub>12</sub>. Additionally, the initial discharge capacity is 165 mA h g<sup>-1</sup> at 0.2 C, which is approaching its theoretical capacity. Chen et al. reported a ball-milling

combined microwave heating method that synthesized  $\text{Li}_4\text{Ti}_5\text{O}_{12}$  as a control sample, the initial capacity of which was  $150 \text{ mA h g}^{-1}$ , and this value decreased relatively quickly [26]. The superiority of our LTO may be attributed to the hydrothermal process that can reduce the particle size of LTO to the nanoscale. The nanosize can effectively improve the contact between the electrolyte and the material so that more capacity can be drawn out successfully [27].

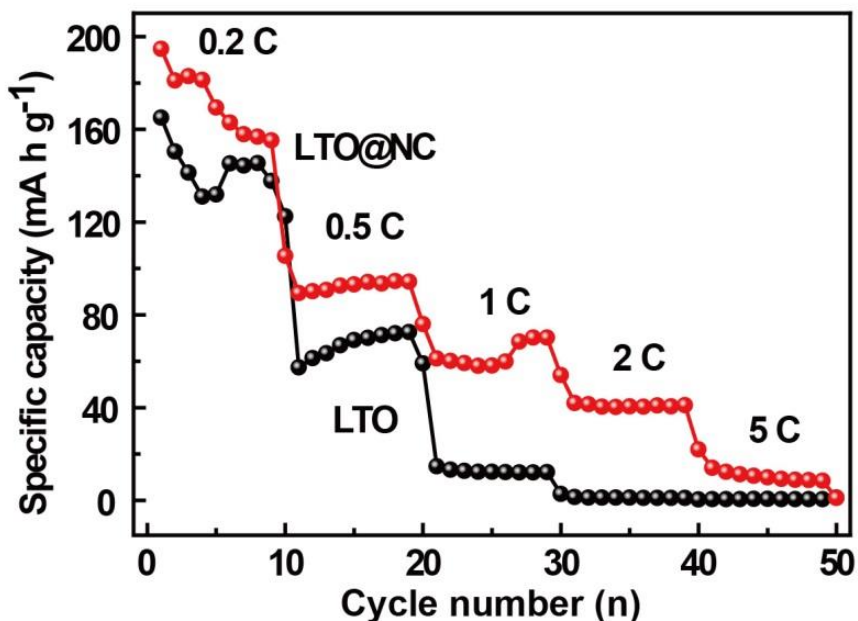


**Figure 4.** The rate performance of LTO and LTO@NC.

Figure 4 compares the rate performance of the pristine LTO and LTO@NC. It is generally accepted that heteroatom (*e.g.*, N, P)-doped materials can provide more active sites, which is favorable for improving the electrochemical performance of materials [2, 9]. As a result, it is well explained that the discharge capacity of LTO@NC under any rate is significantly higher than that of LTO. The initial discharge capacity of LTO@NC can reach  $194.3 \text{ mA h g}^{-1}$ , which is higher than the capacity many works have reported before; a detailed comparison between this work and other recently reported  $\text{Li}_4\text{Ti}_5\text{O}_{12}$ -based anode materials for lithium ion batteries is listed in Table 1. In the following three cycles, the capacity remains at approximately  $181 \text{ mA h g}^{-1}$ , which was higher than the theoretical capacity ( $175 \text{ mA h g}^{-1}$ ). Then, the capacity of LTO@NC stabilizes at approximately  $155 \text{ mA h g}^{-1}$  under 0.2 C, which is close to the works previously reported (Table 1). Under 0.5 C, the discharge capacities of LTO@NC and LTO are approximately  $93 \text{ mA h g}^{-1}$  and  $70 \text{ mA h g}^{-1}$ , respectively, which are 53% and 40% of the theoretical capacities. The capacity retention of LTO under 0.5 C, 1 C, 2 C, and 5 C is 52.4%, 9.3%, 0.8%, and 0.45%, while that of LTO@NC is 55%, 34.3%, 23.9%, and 5.8%, which indicates that the introduction of the N-doped carbon coating layer improved not only the specific capacity but also the rate performance of this material [28].

**Table 1.** Comparison between this work and other recently reported  $\text{Li}_4\text{Ti}_5\text{O}_{12}$ -based anode materials for lithium ion batteries.

Anode Material	Initial Capacity/ mA h g <sup>-1</sup>	Capacity/ mA h g <sup>-1</sup>	Reference
LTO@NC	194.3 (0.2 C)	155 (0.2 C)	This Work
LTO/C	172 (0.2 C)	164 (0.2 C)	[29]
LTO/CNT	162 (0.2 C)	155 (0.2 C)	[26]
LTO/C	170 (0.2 C)	160 (0.2 C)	[30]
BC/LTO	172 (0.2 C)	165 (0.2 C)	[31]
C@LTO	168 (0.1 C)	160 (0.2 C)	[32]
LTO/C-PR	155 (0.2 C)	154 (0.2 C)	[33]

#### 4. CONCLUSIONS

In this work, a hydrothermal method was explored to prepare  $\text{Li}_4\text{Ti}_5\text{O}_{12}$  nanomaterials (LTO), and urea was subsequently used as a carbon and nitrogen source to synthesize a nitrogen-doped carbon-coated  $\text{Li}_4\text{Ti}_5\text{O}_{12}$  (LTO@NC) nanocomposite with a facile method. Therefore, it is broadly proposed to use urea as a carbon and nitrogen source to optimize the electrochemical properties of materials. The results showed that the presence of the N-doped carbon coating layer could form a three-dimensional conductive network, which shortened the diffusion path of electrons, improved the electronic conductivity, and reduced the polarization of the material. In addition, the nanosize of this material after the hydrothermal process was favorable for the infiltration of the electrolyte and shortened the diffusion path of the lithium ions. These two changes synergistically increased the specific capacity and improved the rate performance of LTO@NC.

#### ACKNOWLEDGEMENTS

This work was financially supported by the Fundamental Research Funds for the Central Universities of China (Program No. 2662016QD028, 2662017JC025) and the National Natural Science Foundations of China (Program No. 21603080).

#### References

1. H. Zhang, Q. Deng, C. Mou, Z. Huang, Y. Wang, A. Zhou and J. Li, *Journal of Power Sources*, 239 (2013) 538.
2. H.-G. Jung, S.-T. Myung, C. S. Yoon, S.-B. Son, K. H. Oh, K. Amine, B. Scrosati and Y.-K. Sun, *Energy & Environmental Science*, 4 (2011) 1345.
3. L. Liu, L. Yang, P. Wang, C. Y. Wang, J. Cheng, G. Zhang, J. J. Gu, and F. F. Cao, *International Journal of Electrochemical Science*, 12 (2017) 9844.
4. L. Zhao, Y. S. Hu, H. Li, Z. Wang and L. Chen, *Advanced Materials*, 23 (2011) 1385.
5. H. Li, L. Shen, K. Yin, J. Ji, J. Wang, X. Wang and X. Zhang, *Journal of Materials Chemistry A*, 1 (2013) 7270.
6. G. Hasegawa, K. Kanamori, T. Kiyomura, H. Kurata, K. Nakanishi and T. Abe, *Advanced Energy Materials*, 5 (2015) 1400730.
7. S.-L. Chou, J.-Z. Wang, H.-K. Liu and S.-X. Dou, *The Journal of Physical Chemistry C*, 115 (2011)

- 16220.
8. D. Liu, C. Ouyang, J. Shu, J. Jiang, Z. Wang and L. Chen, *Physica status solidi (b)*, 243 (2006) 1835.
  9. X.-l. Zhang, G.-r. Hu and Z.-d. Peng, *Journal of Central South University*, 20 (2013) 1151.
  10. Y. Wang, H. Liu, K. Wang, H. Eiji, Y. Wang and H. Zhou, *Journal of Materials Chemistry*, 19 (2009) 6789.
  11. M. Krajewski, M. Michalska, B. Hamankiewicz, D. Ziolkowska, K. P. Korona, J. B. Jasinski, M. Kaminska, L. Lipinska and A. Czerwinski, *Journal of Power Sources*, 245 (2014) 764.
  12. B. F. Wang, J. Cao and Y. Liu, *Materials Technology*, 29 (2013) 124.
  13. X. Li, H. C. Lin, W. J. Cui, Q. Xiao and J. B. Zhao, *ACS Applied Materials & Interfaces*, 6 (2014) 7895.
  14. P. Wang, G. Zhang, J. Cheng, Y. You, Y. K. Li, C. Ding, J. J. Gu, X. S. Zheng, C. F. Zhang and F. F. Cao, *ACS Applied Materials & Interfaces*, 9 (2017) 6138.
  15. Y. Wang, W. Zou, X. Dai, L. Feng, H. Zhang, A. Zhou and J. Li, *Ionics*, 20 (2014) 1377.
  16. T. Yuan, R. Cai and Z. Shao, *The Journal of Physical Chemistry C*, 115 (2011) 4943.
  17. W. Fang, X. Cheng, P. Zuo, Y. Ma and G. Yin, *Electrochimica Acta*, 93 (2013) 173.
  18. G.-N. Zhu, H.-J. Liu, J.-H. Zhuang, C.-X. Wang, Y.-G. Wang and Y.-Y. Xia, *Energy & Environmental Science*, 4 (2011) 4016.
  19. N. Li, G. Zhou, F. Li, L. Wen and H.-M. Cheng, *Advanced Functional Materials*, 23 (2013) 5429.
  20. Z. Zhang, G. Li, H. Peng and K. Chen, *Journal of Materials Chemistry A*, 1 (2013) 15429.
  21. H. Pan, L. Zhao, Y. S. Hu, H. Li and L. Chen, *ChemSusChem*, 5 (2012) 526.
  22. C. Lai, Y. Y. Dou, X. Li and X. P. Gao, *Journal of Power Sources*, 195 (2010) 3676.
  23. Z. Ding, L. Zhao, L. Suo, Y. Jiao, S. Meng, Y. S. Hu, Z. Wang and L. Chen, *Physical chemistry chemical physics : PCCP*, 13 (2011) 15127.
  24. Y.-R. Zhu, P. Wang, T.-F. Yi, L. Deng and Y. Xie, *Solid State Ionics*, 276 (2015) 84.
  25. C. Han, Y. B. He, B. Li, H. Li, J. Ma, H. Du, X. Qin, Q. H. Yang and F. Kang, *ChemSusChem*, 7 (2014) 2567.
  26. Y. Chen, H. Zhang, Y. Li, Y. Chen, T. Luo, *International Journal of Hydrogen Energy*, 42 (2017) 7195.
  27. W. J. H. Borghols, M. Wagemaker, U. Lafont, E. M. Kelder and F. M. Mulder, *Journal of the American Chemical Society*, 131 (2009) 17786.
  28. H. Li, L. Shen, K. Yin, J. Ji, J. Wang, X. Wang and X. Zhang, *Journal of Materials Chemistry A*, 1 (2013) 7270.
  29. Y. Ren, P. Lu, X. Huang, S. Zhou, Y. Chen, B. Liu, F. Chu, J. Ding, *Solid State Ionics*, 274 (2015) 83.
  30. H. Luo, L. Shen, K. Rui, H. Li, X. Zhang, *Journal of Alloys and Compounds*, 572 (2013) 37.
  31. G. Luo, J. He, X. Song, X. Huang, X. Yu, Y. Fang, D. Chen, *Journal of Alloys and Compounds*, 621 (2015) 268.
  32. Q. Cheng, S. Tang, J. Liang, J. Zhao, Q. Lan, C. Liu and Y.-C. Cao, *Results in Physics*, 7 (2017) 810.
  33. X. Li, J. Xu, P. Huang, W. Yang, Z. Wang, M. Wang, Y. Huang, Y. Zhou, M. Qu, Z. Yu and Y. Lin, *Electrochimica Acta*, 190 (2016) 69.